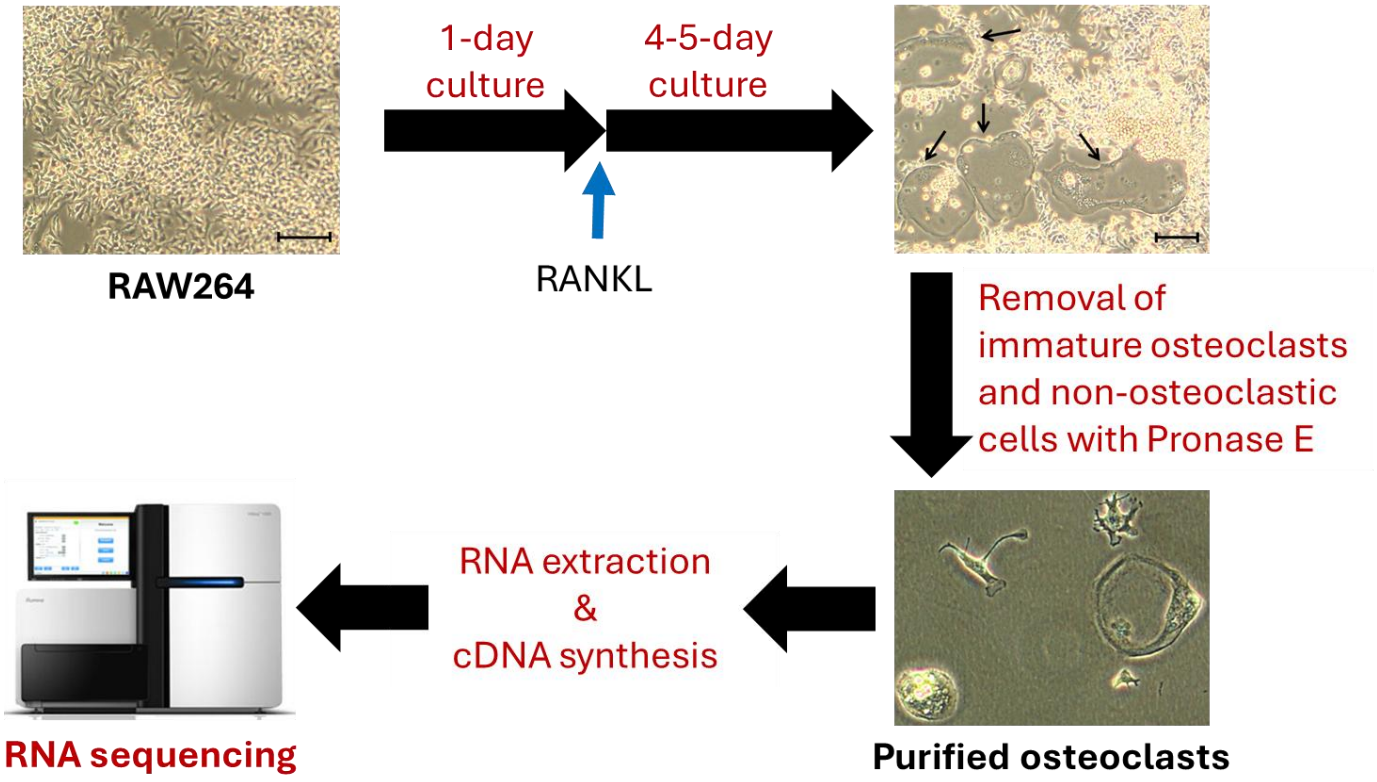

Supplementary Figure 1. Scheme of the bulk RNA sequencing of mouse osteoclasts differentiated from RAW264 cells

Supplementary Figure S1

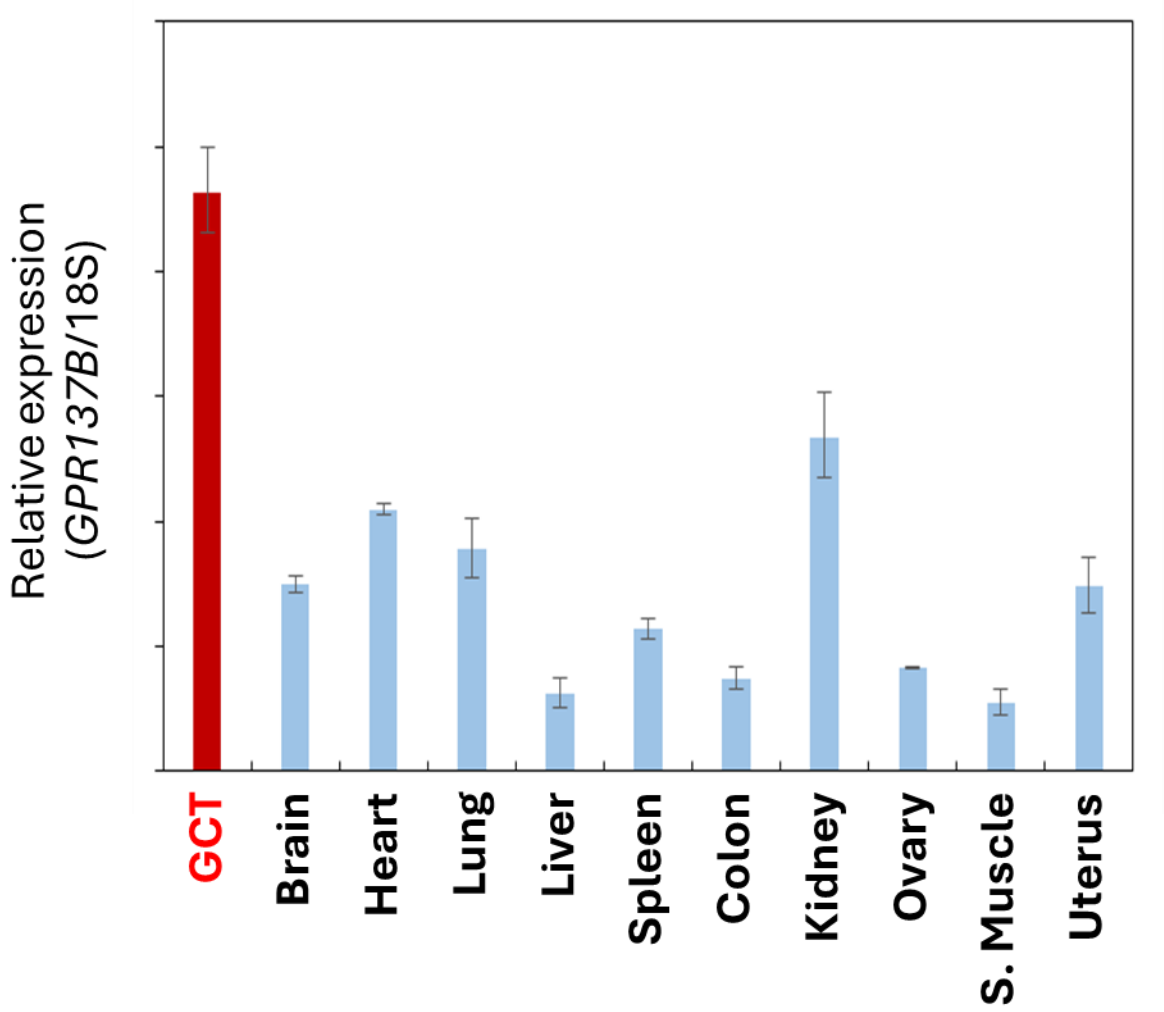

Supplementary Figure S2. Dominant *Gpr137b* mRNA expression in human Giant cell tumor of bone (GCT)

Supplementary Figure S2

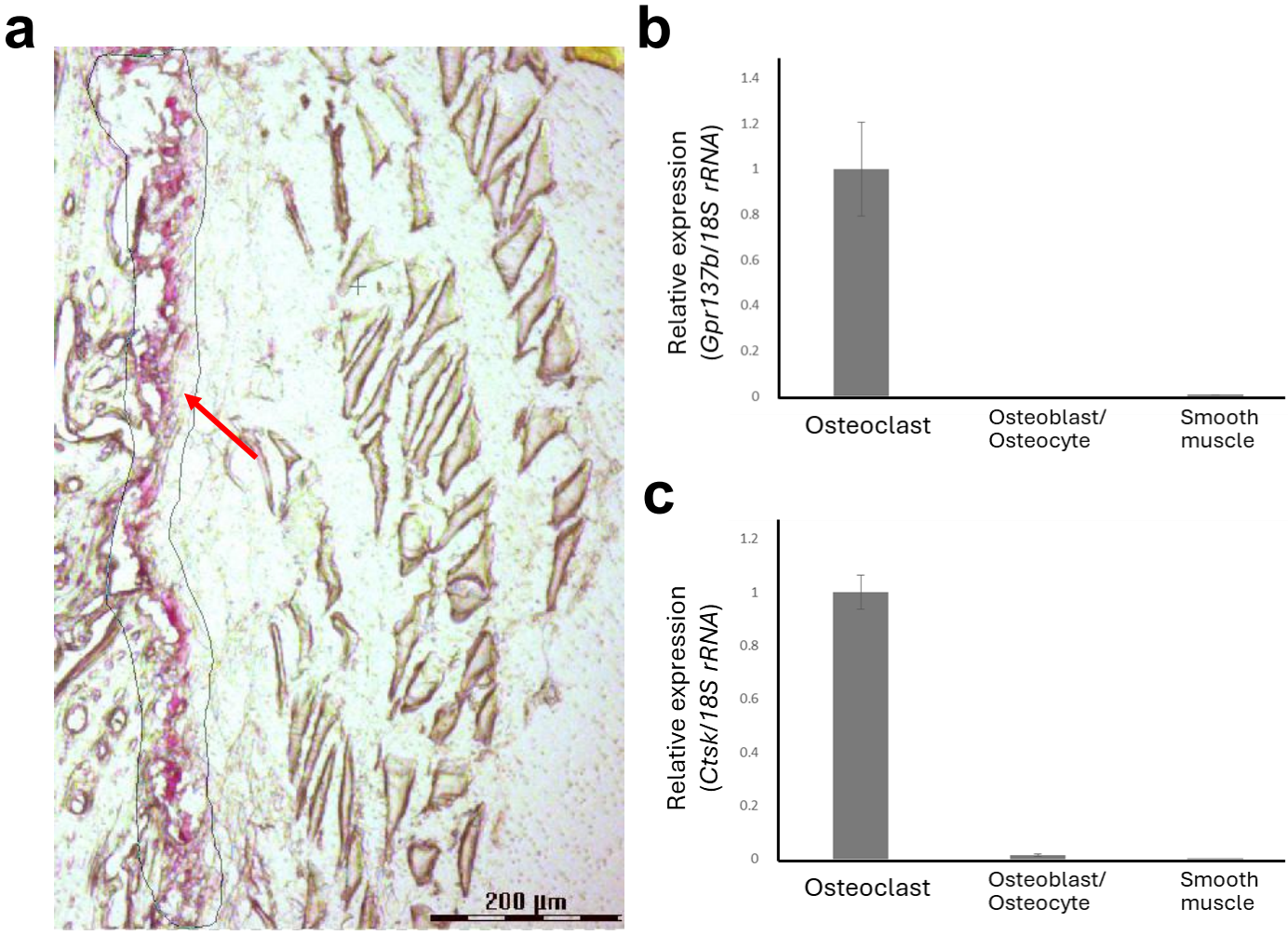

Supplementary Figure S3. Abundant *Gpr137b* mRNA expression in the osteoclast-rich region compared to the adjacent osteoblasts/osteocytes- and smooth muscle-rich regions of the laser-dissected mouse femur sections. (a) Regions rich in TRAP-positive osteoclasts in the femur (indicated by an arrow) was dissected. (b) The expression of *Gpr137b* mRNA normalized to 18S rRNA was evaluated by qRT-PCR. (c) The expression of *Gpr137b* mRNA normalized to *18S rRNA* was evaluated by qRT-PCR.

Supplementary Figure S3

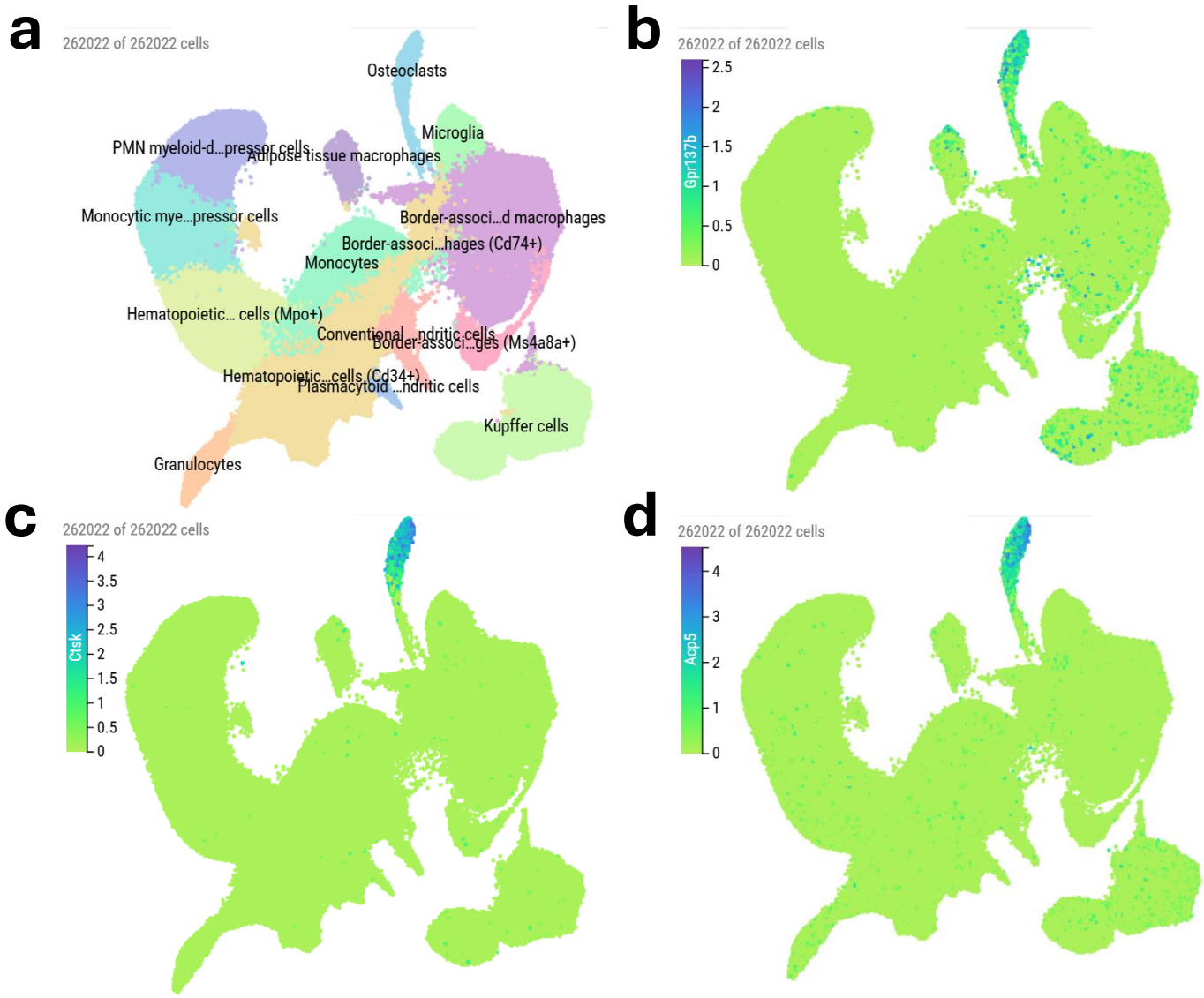

Supplementary Figure S4. UMAP-based visualization of the CZ CELLxGENE single-cell dataset of white blood cells from mouse embryos. In the UMAP projection with annotated cell clusters (a), the expression of *Gpr137b* (b) as well as *Ctsk* (c) and *Acp5* (d) mRNAs was shown to be localized in the cluster annotated as 'osteoclast'.

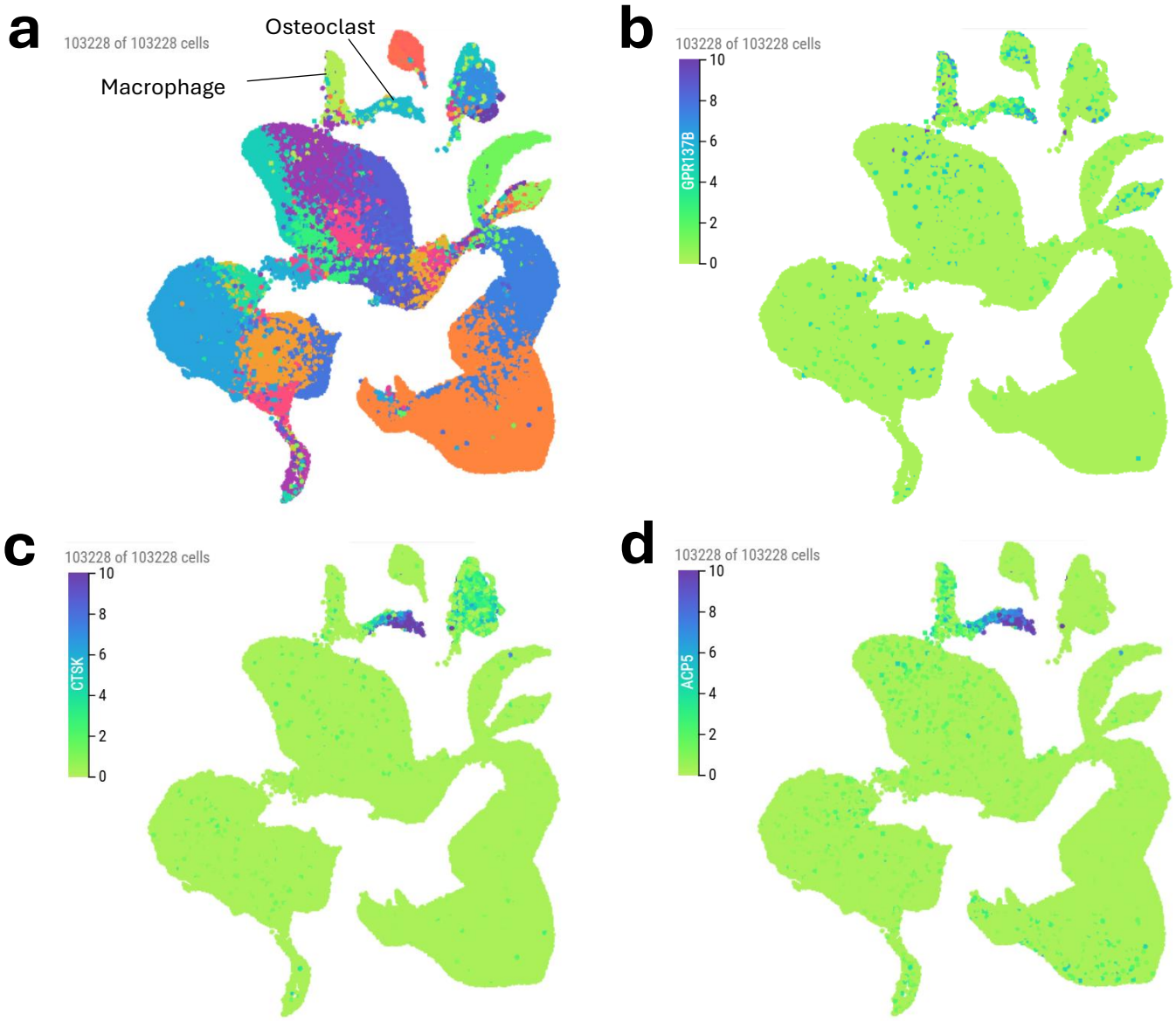

Supplementary Figure S5 UMAP-based visualization of the CZ CELLxGENE single-cell dataset of white blood cells from human bone marrow cells. In the UMAP projection with annotated cell clusters (a), the expression of *Gpr137b* (b) as well as *Ctsk* (c) and *Acp5* (d) mRNAs was shown to be localized in the cluster annotated as 'osteoclast'.

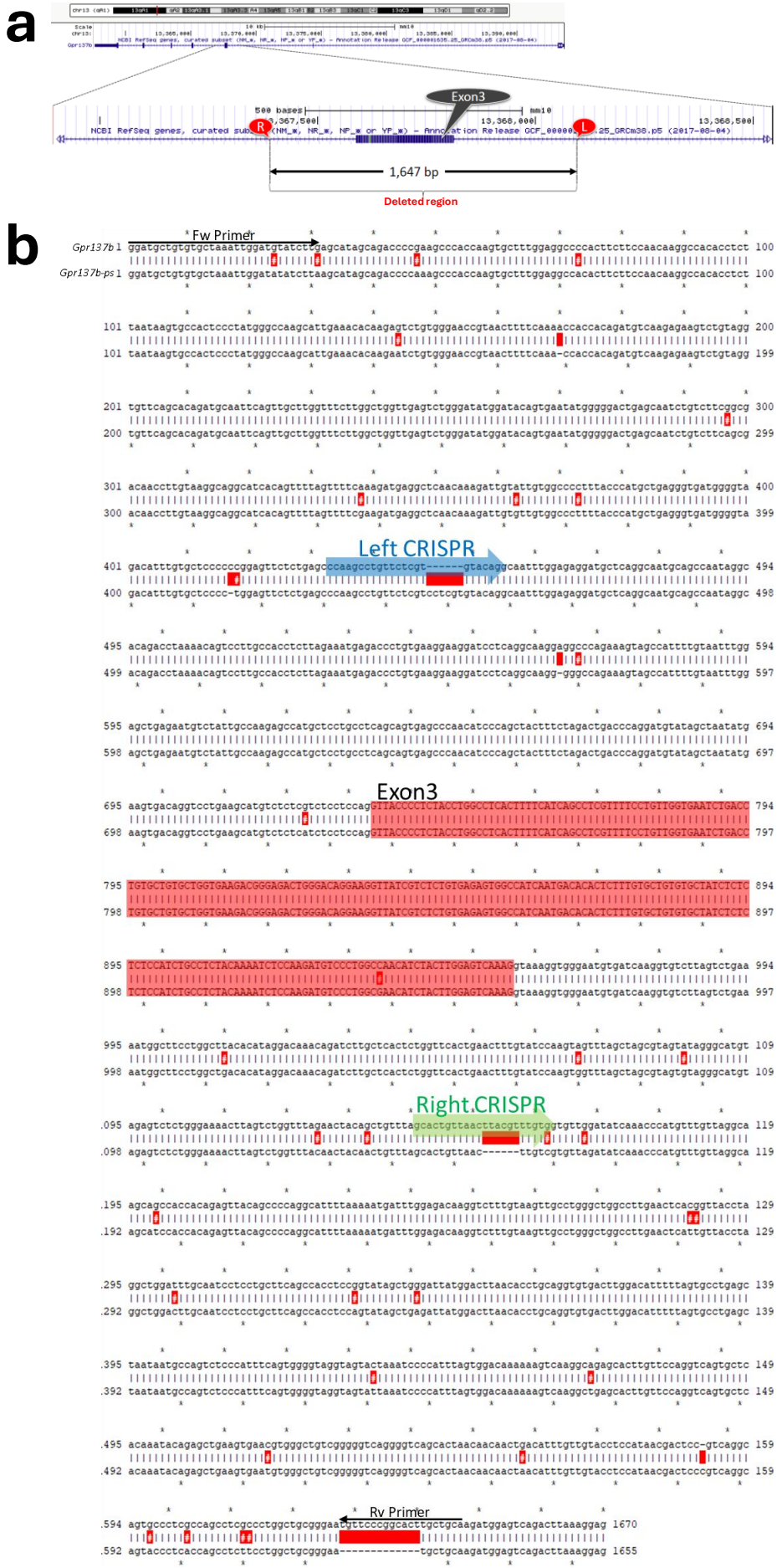

Supplementary Figure S6

Supplementary Figure S6. Crispr/Cas9-based deletion of the *Gpr137b* gene in the mouse genome. (a) The exon 3-containing region deleted in the mouse *Gpr137b* gene locus. (b) The nucleotide sequence alignment of the *Gpr137b* exon 3-containing region with the corresponding region of the mouse *Gpr137b-ps* gene.

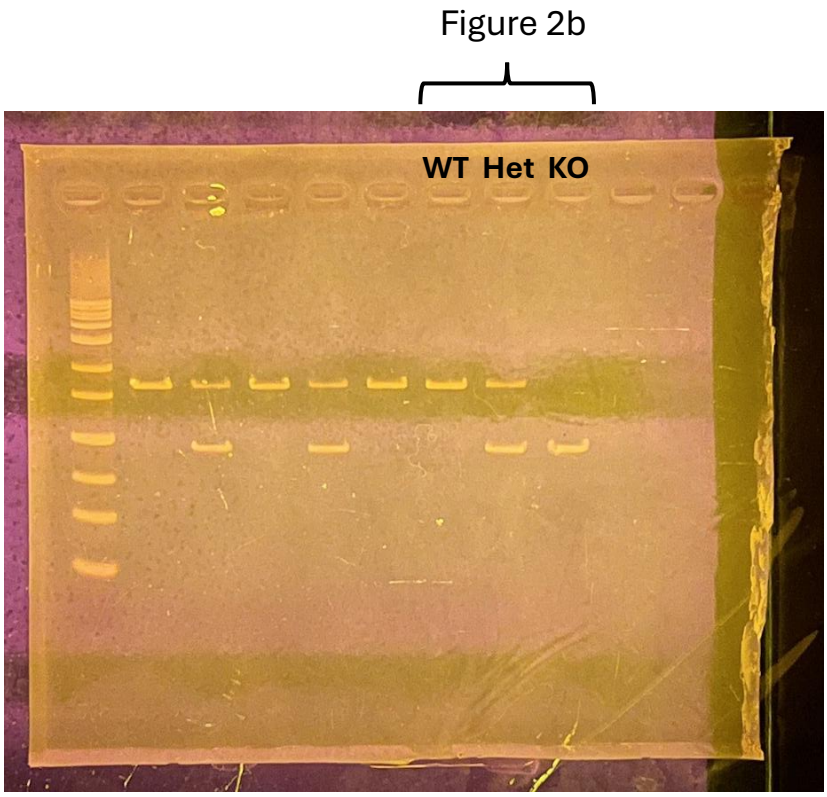

Supplementary Figure S7. Original gel image for Figure 2b.

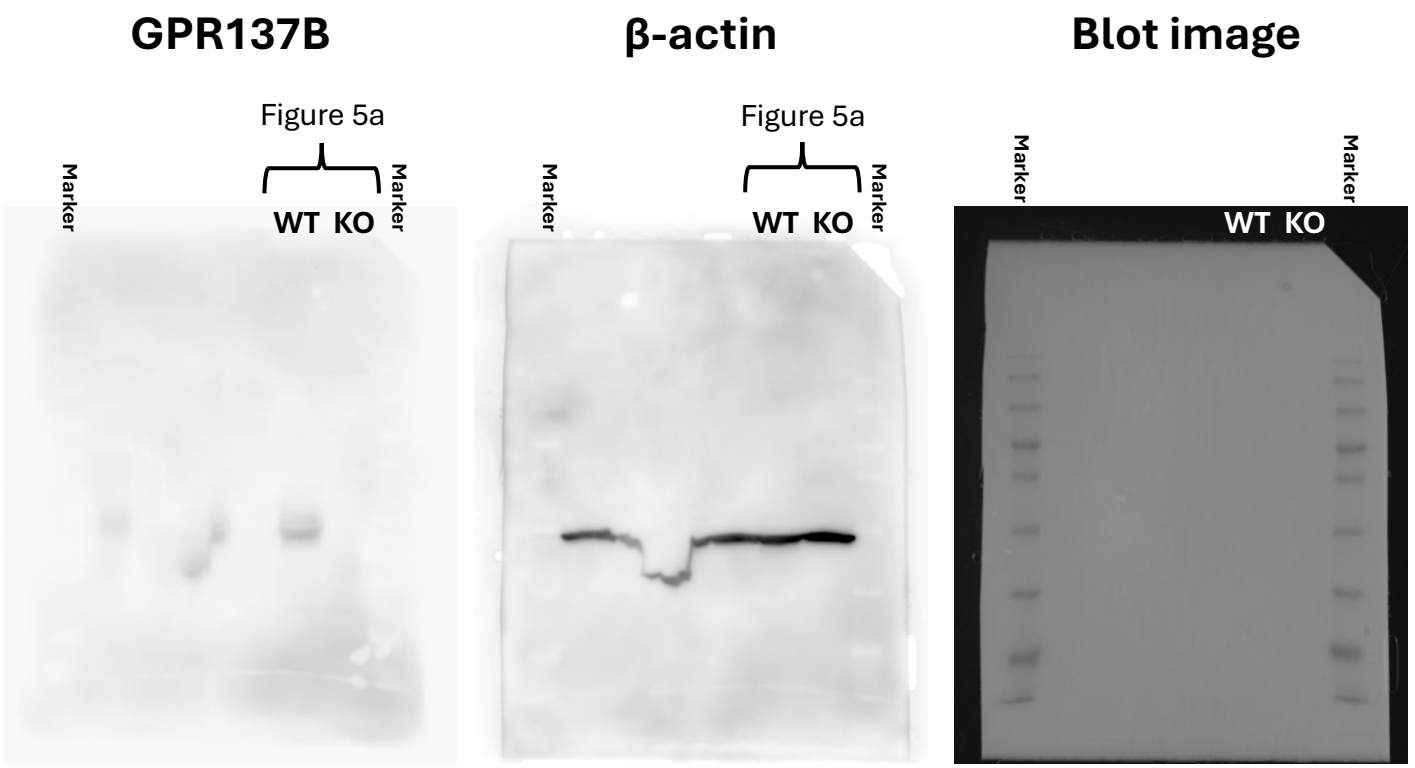

Supplementary Figure S8. Original western blot image for Figure 5a. The western blot probed with the anti-mouse GPR137B antibody was stripped and reprobed with the anti-mouse β-actin antibody.

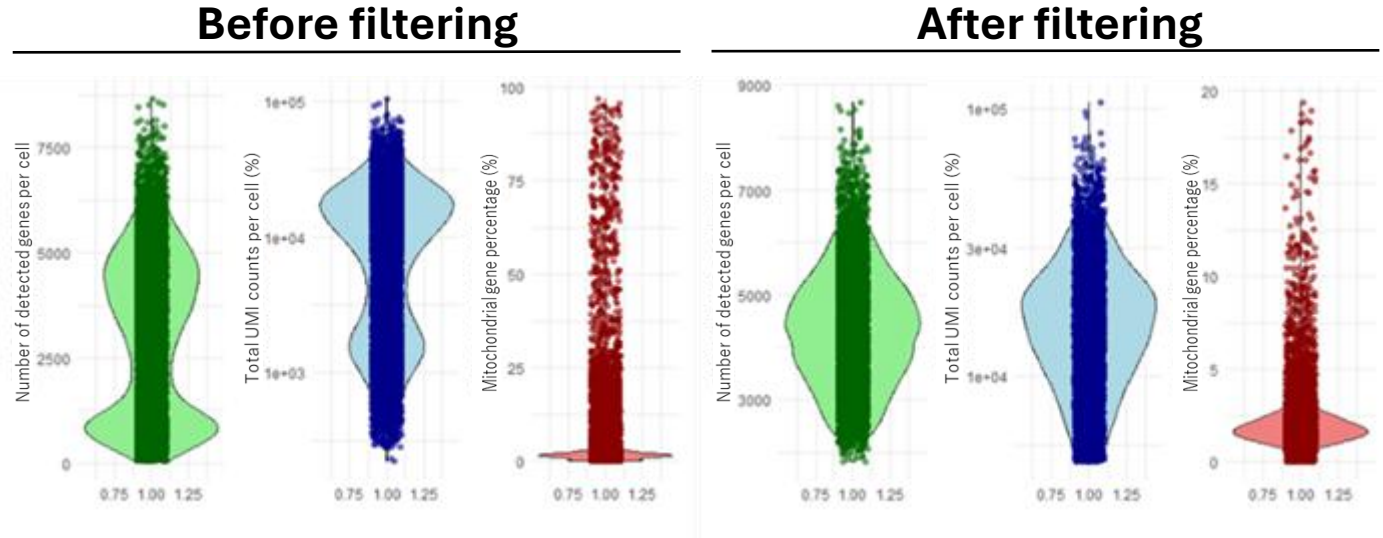

Supplementary Figure S9. Quality control metrics before and after filtering in the single-cell RNA sequencing data.

Supplementary Figure S7

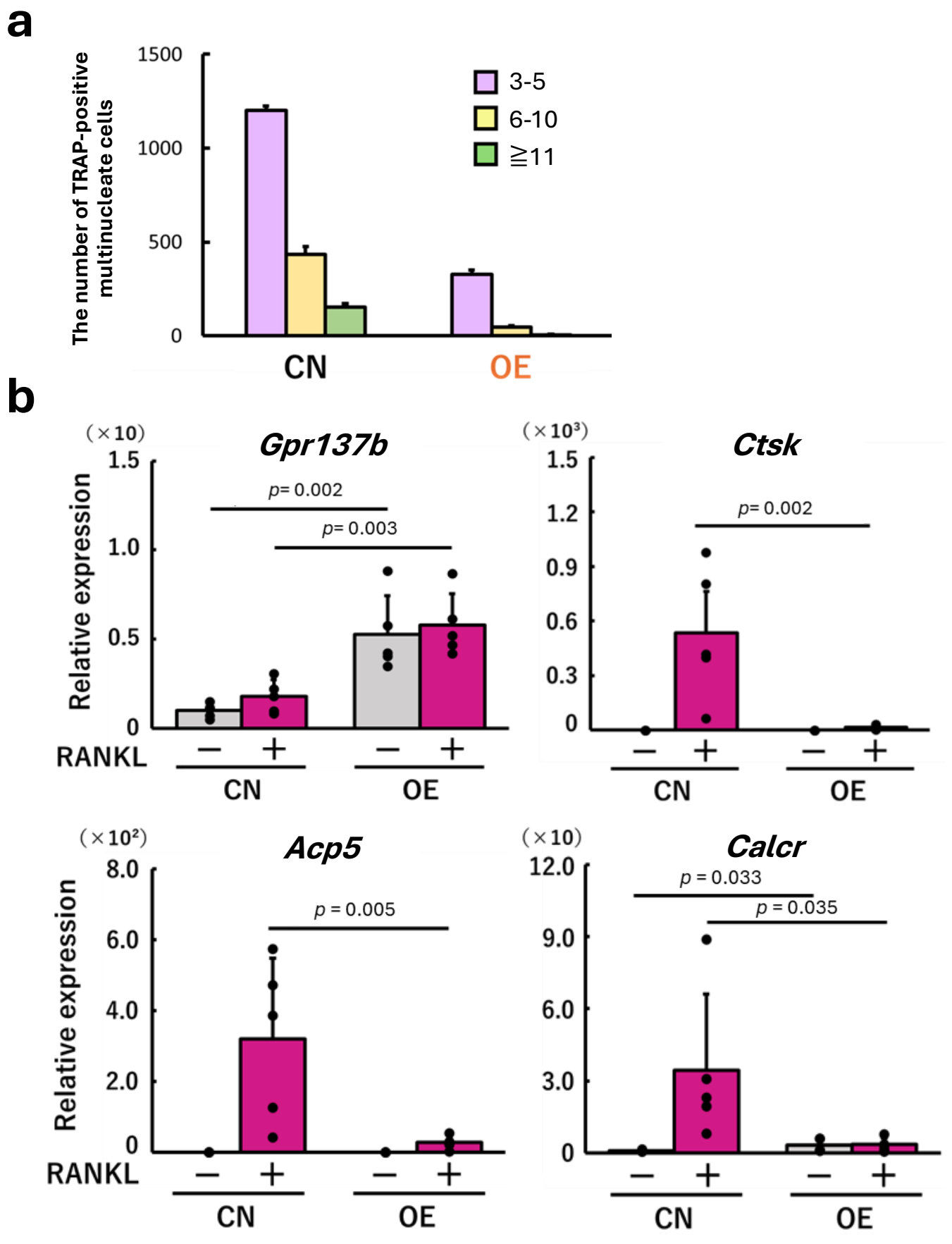

Supplementary Figure S8

Supplementary Figure S10. RANKL-induced osteoclastic differentiation of RAW264 cells with the adenovirus-mediated overexpression of *Gpr137b*. (a) The number of multinucleate TRAP-positive cells with the nucleus numbers of 3-5, 6-10, and ≧11, which correspond to small-, middle-and large-sized osteoclasts, respectively. (b) qRT-PCR analyses to evaluate the expression levels of *Gpr137b* and representative osteoclast marker genes (*Acp5*, *Ctsk*, and *Calcr*) in the *Gpr137b*-overexpresing (OE) and control (CN) RAW264 cells treated with or without RANKL.

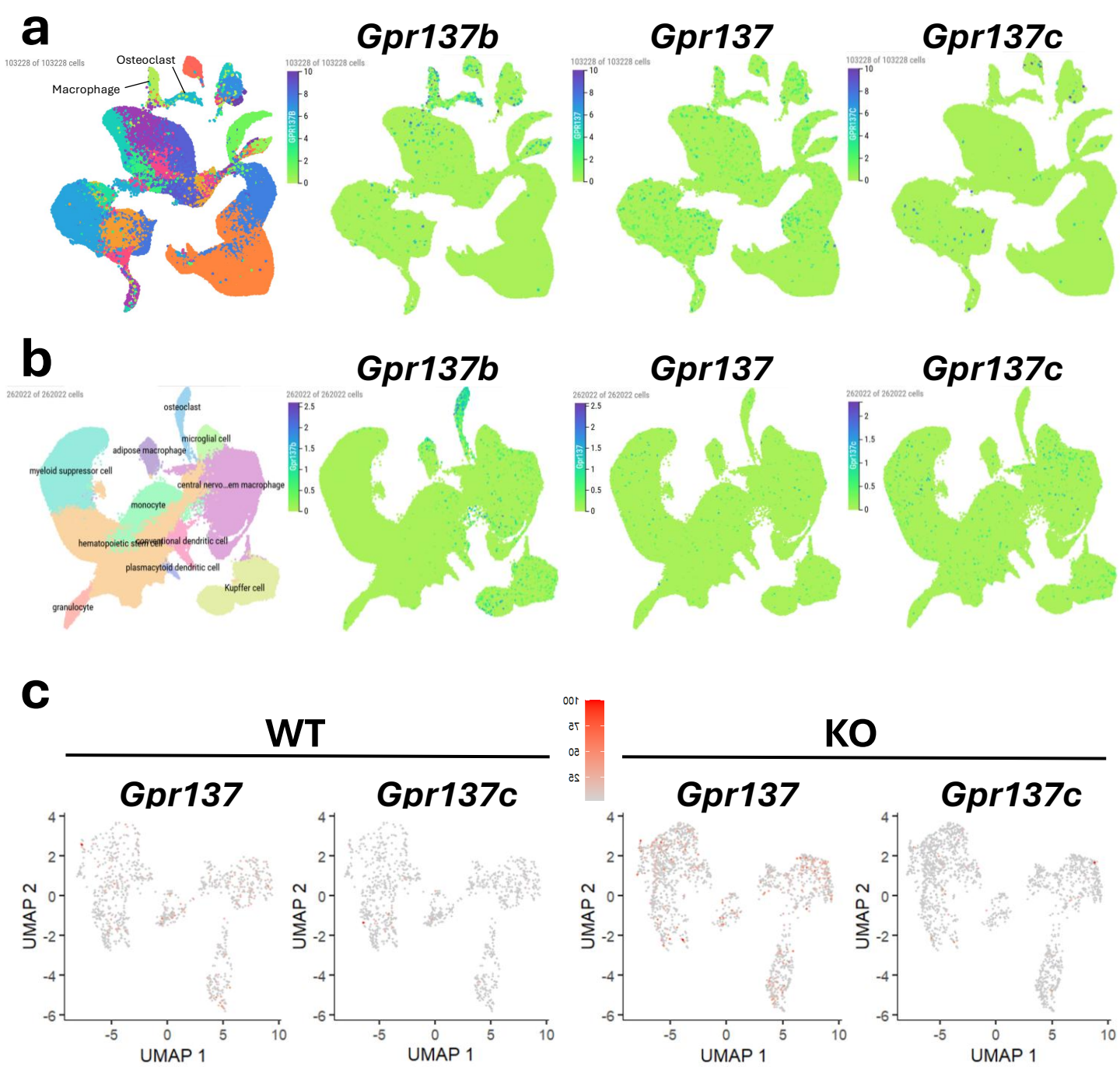

Supplementary Figure S11. Heatmaps visualizing the expression of *Gpr137b* homologues in single-cell clusters on UMAP. Heatmaps visualizing *Gpr137b*, *Gpr137* and *Gpr137c* mRNA expression in the clusters of human bone marrow-derived cell types (a) and mouse white blood cell-derived cell types (b) including osteoclast, based on the CZ CELLxGENE single-cell analysis dataset. (c) Heatmaps visualizing *Gpr137* and *Gpr137c* mRNA expression in the cell type clusters of mouse bone marrow-derived cells, including osteoclast, from the *Gpr137b*-WT and KO mice.

Supplementary Figure S9